

Efficacy Versus Hepatotoxicity of High-dose Rifampin, Pyrazinamide, and Moxifloxacin to Shorten Tuberculosis Therapy Duration: There Is Still Fight in the Old Warriors Yet!

Shashikant Srivastava, Devyani Deshpande, Gesham Magombede, and Tawanda Gumbo[✉]

Center for Infectious Diseases Research and Experimental Therapeutics, Baylor Research Institute, Baylor University Medical Center, Dallas, Texas

Background. One approach that could increase the efficacy and reduce the duration of antituberculosis therapy is pharmacokinetics/pharmacodynamics-based optimization of doses. However, this could increase toxicity.

Methods. We mimicked the concentration-time profiles achieved by human equivalent doses of moxifloxacin 800 mg/day, rifampin 1800 mg/day, and pyrazinamide 4000 mg/day (high-dose regimen) vs isoniazid 300 mg/day, rifampin 600 mg/day, and pyrazinamide 2000 mg/day (standard therapy) in bactericidal and sterilizing effect studies in the hollow fiber system model of tuberculosis (HFS-TB). In an intracellular *Mycobacterium tuberculosis* (*Mtb*) HFS-TB experiment, we added a 3-dimensional human organotypic liver to determine potential hepatotoxicity of the high-dose regimen, based on lactate dehydrogenase (LDH). Treatment lasted 28 days and *Mtb* bacterial burden was based on colony counts. We calculated the time to extinction (TTE) of the *Mtb* population in the HFS-TB and used morphism-based transformation and Latin hypercube sampling to identify the minimum therapy duration in patients.

Results. The kill rate of standard therapy in the bactericidal effect and sterilizing effect experiments were 0.97 (95% confidence interval [CI], .91–.99) \log_{10} colony-forming units (CFU)/mL/day, and 0.56 (95% CI, .49–.59) \log_{10} CFU/mL/day, respectively. The high-dose regimen's bactericidal and sterilizing effect kill rates were 0.99 (95% CI, .96–.99) \log_{10} CFU/mL/day and 0.72 (95% CI, .56–.79) \log_{10} CFU/mL/day, respectively. The upper confidence bound for TTE in patients was 4.5–5 months for standard therapy vs 3.7 months on the high-dose regimen. There were no differences in LDH concentrations between the 2 regimens at any time point ($P > .05$).

Conclusions. The high-dose regimen may moderately shorten therapy without increased hepatotoxicity compared to standard therapy.

Keywords. 3D liver; liver toxicity; mathematical modeling; time to extinction; hollow fiber system model.

There are compelling reasons to create new treatment regimens for tuberculosis (TB) that are of shorter duration than the current 6-month regimen for drug-susceptible TB, which could also form the backbone of treatment of multidrug-resistant TB (MDR-TB) [1]. The trick is to accelerate sterilizing effect against extracellular tubercle bacilli, as well as to kill intracellular bacteria [2]. One approach is to use principles of pharmacokinetics/pharmacodynamics (PK/PD) to find the exposures of standard anti-TB agents that maximally kill *Mycobacterium tuberculosis* (*Mtb*), and then give patients doses that achieve those exposures. A second approach is the discovery of new pharmacophores such as bicyclic nitroimidazopyrans and

bedaquiline, which could shorten therapy duration in MDR-TB [3, 4]. A third approach is repurposing older antibiotics for use in MDR-TB and drug-susceptible TB, as has been the case with fluoroquinolones, oxazolidinones, carbapenems, penems, benzylpenicillin, cephalosporins, and clofazimine [5–10]. Here, we used a combination of these approaches.

Two fluoroquinolones (moxifloxacin and gatifloxacin) dosed at the currently recommended dose of 400 mg/day failed to shorten therapy duration in recent studies [11, 12]. One possible reason could be concentration-dependent antagonism, seen with quinolones such as gatifloxacin and moxifloxacin, noted in the accompanying article in this supplement [13]. This problem could be overcome by optimizing the doses of the fluoroquinolones and rifampin [13–17]. Indeed, hollow fiber system model of TB (HFS-TB) PK/PD studies, along with clinical studies, suggest increasing the dose of rifampin at least 3-fold and pyrazinamide at least 2-fold in the treatment of drug-susceptible TB [15, 18, 19]. Forty years ago, Kreis et al administered a 3-month regimen of rifampin 1200 mg per day,

Correspondence: T. Gumbo, Center for Infectious Diseases Research and Experimental Therapeutics, Baylor Research Institute, 3434 Live Oak St, Dallas, TX 75204 (tawanda.gumbo@BSWhealth.org).

Clinical Infectious Diseases® 2018;67(S3):S359–64

© The Author(s) 2018. Published by Oxford University Press for the Infectious Diseases Society of America. All rights reserved. For permissions, e-mail: journals.permissions@oup.com. DOI: 10.1093/cid/ciy627

isoniazid 900 mg per day, and streptomycin 1 g per day, which had an almost perfect sputum conversion at the end of the therapy, and relapse rates of only 11% [20]. This is similar to the relapse rates in the recent 4-month fluoroquinolone regimens; what is remarkable is that the Kreis regimen did not have pyrazinamide, which is an important driver of sterilizing effect in standard therapy [4, 11, 21]. On the other hand, isoniazid has concentration-dependent antagonism with rifampin and pyrazinamide, and is the least contributive of sterilizing effect [21, 22]. In contrast, rifampin is synergistic with pyrazinamide in a concentration-dependent fashion [23]. Therefore, we investigated a high-dose-based rifampin and pyrazinamide regimen in which isoniazid was replaced with high-dose moxifloxacin to determine if sterilizing effect rates were faster than with standard therapy, and thus lead to shorter therapy duration.

Concerns of high-dose use of anti-TB drugs have centered on potential toxicity, especially hepatotoxicity [23, 24]. In recent years we introduced a 3-dimensional (3D) organotypic liver module to the HFS-TB, which has allowed us to assess for possible hepatotoxicity of anti-TB drugs [25]. This allows us to identify both efficacy and hepatotoxicity from the same HFS-TB units. Here, we used this model to determine potential hepatotoxicity of the high-dose regimen compared to standard therapy.

Finally, preclinical studies have had a poor record of accurately identifying shorter therapy durations that could be used in the clinic [4, 11, 26]. Therefore, we have developed mathematical and computational models to predict the time to extinction (TTE) of the total bacterial population (“cure” by standard definition) starting in the HFS-TB to the clinic [27]. We used these models to determine the optimal duration of the therapy with the high-dose regimen, based on TTE.

MATERIALS AND METHODS

Drugs and Supplies

Isoniazid, rifampin, and pyrazinamide were purchased from Sigma-Aldrich, while moxifloxacin was purchased from our campus pharmacy. Hollow fiber cartridges were purchased from FiberCell (Frederick, Maryland). 3D liver organoid “KUBES” were procured from Kiyatec Inc (Greenville, South Carolina). A commercially available kit (ab102526) from Abcam (Cambridge, Massachusetts) was used to measure the liver enzyme lactate dehydrogenase (LDH).

Bacterial Strain and Growth Conditions

Stock culture of *Mtb* (H37Ra, American Type Culture Collection [ATCC] 25177 and *Mtb* H37Rv, ATCC 27294) were thawed and grown in Middlebrook 7H9 broth supplemented with 10% oleic acid-dextrose-catalase at 37°C under 5% carbon dioxide (CO₂) and shaking conditions prior to each experiment. To produce semidormant bacilli, log-phase growth *Mtb* was subcultured for 4 more days in Middlebrook 7H9 broth acidified and buffered to a pH of 5.8, as described previously [28].

Tissue Culture

Human-derived monocyte cells (THP-1; ATCC TIB-202) were grown in RPMI 1640 medium supplemented with 10% fetal bovine serum at 37°C under 5% CO₂. The THP-1 cells were subcultured every 4 days. Prior to each experiment, cells were checked for mycoplasma contamination using the e-Myco-Mycoplasma polymerase chain reaction detection kit (version 2.0; iNtron Biotechnology). Any bacterial contamination was ruled out by plating a portion of the cell culture on Muller-Hinton agar. The culture conditions of the HepG2 cells in the 3D KUBES were the same as described previously [25].

Hollow Fiber Models of Bactericidal Effect, Sterilizing Effect, and Hepatotoxicity

The HFS-TB for bactericidal effect, which utilizes 4 day old log-phase growth cultures, has been described in detail previously and in the introduction to this supplement [15, 18, 29]. The details of the HFS-TB for sterilizing effect, in which *Mtb* growth is 10- to 20-fold slower than log-phase growth, have also been described in detail in the past [30]. The HFS-TB for intracellular *Mtb* has also been described in previous publications, including the methods of co-culture with a 3D KUBES to examine hepatotoxicity [25]. Each of these models allows administration of multiple drug therapy to recapitulate the drug concentration-time profiles as encountered in humans, as well as examination of microbial kill of *Mtb* in each of the specified physiologic states believed to be encountered in patients [31].

Combination Therapy Regimens Examined in the HFS-TB

We performed (1) bactericidal, (2) sterilizing activity, and (3) intracellular *Mtb* HFS-TB studies in which we treated HFS-TB replicates with standard therapy and a regimen of high-dose moxifloxacin, rifampin, and pyrazinamide (high-dose regimen). The target drug peak concentration (C_{max}) and 0- to 24-hour area under the concentration-time curve (AUC_{0-24}) and PK/PD exposure for each drug are shown in Table 1. There were 3 HFS-TB replicates for each regimen. All drugs were infused via a computer-controlled syringe pump, and the different half-lives and peak concentrations of each drug were recapitulated within the same HFS-TB unit. The central compartment was sampled at 8 different time points over 24 hours to measure the drug concentrations. The peripheral compartment of each of the HFS-TB was sampled on days 0, 7, 14, 21, and 28 to enumerate the total bacterial burden as well as to determine the proportion of the drug-resistant subpopulations by culturing on Middlebrook 7H10 agar supplemented with 3 times the minimum inhibitory concentration (MIC) of each drug. In the intracellular HFS-TB model, samples were collected from the central compartment on days 0, 7, 14, 21, and 28 and used to measure the levels of LDH as surrogate of the hepatotoxicity.

Pharmacokinetic Modeling

We utilized multiplexed assays for measurement of drug concentrations of moxifloxacin, rifampin, isoniazid, and pyrazinamide,

Table 1. Human Equivalent Dose of the Drugs Used in the Hollow Fiber System Model of Tuberculosis Studies and the Intended Versus Achieved Drug Exposures

Regimen	Dose	Intended			Achieved			
		C _{max} , mg/L	AUC ₀₋₂₄ , mg × h/L ⁻¹	MIC	C _{max} , mg/L	AUC ₀₋₂₄ , mg × h/L ⁻¹	C _{max} /MIC	AUC ₀₋₂₄ /MIC
Standard therapy								
Isoniazid	10 mg/kg/d	6	22	0.06	5.02	25.57	83.67	426.17
Rifampin	10 mg/kg/d	6.8	24	0.06	6.26	27.57	104.33	459.50
Pyrazinamide	25 mg/kg/d	54	390	25	48.63	297.4	1.95	11.90
High-dose regimen								
Rifampin	30 mg/kg/d	18	66	0.06	18.69	83.44	311.50	1390.67
Pyrazinamide	50 mg/kg/d	108	780	25	96.3	774.5	3.85	30.98
Moxifloxacin	800 mg/d	8.4	90	0.12	7.64	84.22	63.67	701.83

Abbreviations: AUC₀₋₂₄, 0- to 24-hour area under the concentration–time curve; C_{max}, maximum concentration; MIC, minimum inhibitory concentration.

as described in detail previously [15, 25]. Pharmacokinetic modeling was performed for each drug as described in the past, using ADAPT 2 software of D'Argenio et al [25, 32, 33]. The isoniazid, rifampin, pyrazinamide, and moxifloxacin MICs used for these exposure calculations were those reported in our previous publication and are listed in Table 1 [15, 34]. These were used to calculate observed AUC₀₋₂₄/MICs and C_{max}/MICs.

Time-to-Extinction Modeling

First, the growth rates of different *Mtb* subpopulations (log-phase growth, intracellular, or semidormant) were calculated using the nontreated HFS-TB system colony-forming units (CFU)/mL (controls). Second, the kill rates of each population with standard or high-dose regimens were calculated using equations described elsewhere in this supplement [27]. Third, we mapped these HFS-TB values to the patients to translate TTE of each bacterial subpopulation. We performed in silico clinical trial simulations using the Latin hypercube sampling method to simulate the outcomes in 1000 patients, and mapping transformations to predict the TTE in patients treated with either regimen, as described in detail elsewhere in the supplement [27, 35]. We calculated the proportion of patients cured after 3, 4, and 6 months of therapy to determine if the high-dose regimen can shorten the therapy duration.

RESULTS

Concentration-Time Profiles and Drug Exposures Achieved in the HFS-TB

The concentration-time profiles of isoniazid, rifampin, pyrazinamide, and moxifloxacin, achieved in the central compartment of each HFS-TB replicate in each experiment in each regimen, were combined for purposes of reporting and are shown in Supplementary Figure 1A–D. Pharmacokinetic modeling of these data revealed the AUC₀₋₂₄, AUC₀₋₂₄/MIC, C_{max}, and C_{max}/MIC (Table 1). For the standard regimen, the values were on the high end of the distribution identified in patients on treatment for drug-susceptible TB in the Western Cape, which means that standard therapy regimens were actually optimized for 2 of the 3 drugs in Table 1, and were on the maximal kill (E_{max}) and fast sputum conversion portion of the dose-response curve

[18, 36–38]; for the experimental regimen, the values were 2–3 times higher, as was intended [38].

Intracellular HFS-TB Studies for Efficacy and Hepatotoxicity

The number of the viable THP-1 cells in the HFS-TB that received either standard-dose combination or high-dose combination or received no treatment at all, did not differ at any given time point (Figure 1A). This suggests that the high dose of rifampin and pyrazinamide were not toxic to the THP-1 human monocytes. Figure 1B shows the LDH concentrations in the intracellular HFS-TB model with 3D KUBES at each sampling time point. The changes in the LDH levels between the standard regimen and high-dose regimen were not statistically different by *t* test, performed for each sampling time point (*P* > .05).

TTE of *Mtb* With Standard and High-dose Regimens

Supplementary Figure 2 shows the growth rate of *Mtb* in the nontreated HFS-TB for each bacterial subpopulation (intracellular, log-phase, and slowly growing bacteria). As shown in Supplementary Figure 2A, *Mtb* in log-phase or intracellular environment had similar growth rates (0.33 [95% confidence interval {CI}, .15–.63] log₁₀ CFU/mL/day), hence we combined the data for graphing. The growth rate of *Mtb*, growing under acidic conditions, in the sterilizing activity experiments (Supplementary Figure 2B) was 0.19 (95% CI, .14–.23) log₁₀ CFU/mL/day.

The kill rates of *Mtb* with standard therapy and the high-dose regimen are shown in Figure 2A and 2B, respectively. Figure 2A shows that the kill rates for the log-phase growth and intracellular *Mtb* with both the standard and the high-dose regimen were not significantly different from each other (0.97 [95% CI, .91–.99] log₁₀ CFU/mL/day vs 0.99 [95% CI, .96–.99] log₁₀ CFU/mL/day, respectively). The kill rate of the high-dose regimen in the sterilizing activity studies was 0.72 (95% CI, .56–.79) log₁₀ CFU/mL/day compared to the 0.56 (95% CI, .49–.59) log₁₀ CFU/mL/day kill rate of the standard regimen (Figure 2B).

These kill rates were then used to transform the HFS-TB data to the patients to determine the TTE of each regimen, as detailed elsewhere [27]. Figure 2C shows that based on the

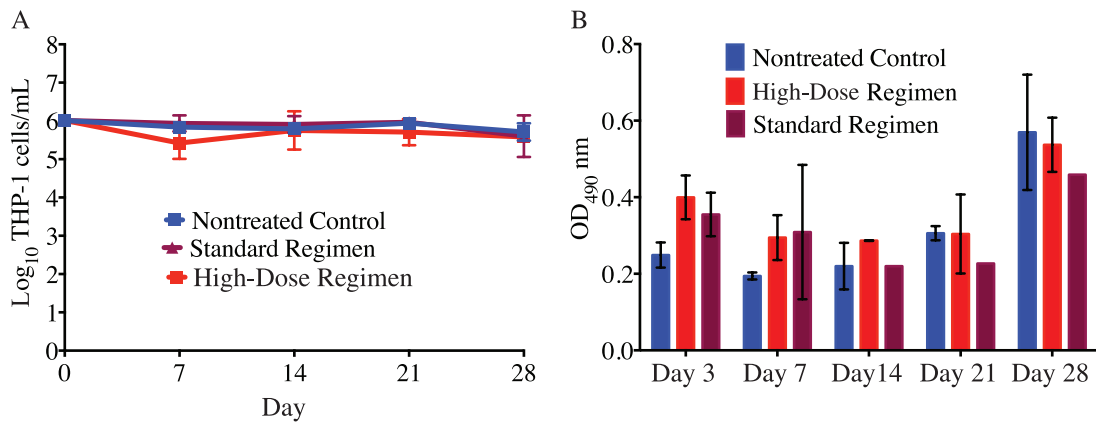


Figure 1. Viability of the THP-1 cells and level of lactose dehydrogenase (LDH). *A*, The number of viable THP-1 cells did not differ between the standard treatment regimen and the high-dose regimen ($P > .05$). *B*, On days 3 and 7, the LDH concentrations were higher in both the standard-therapy and high-dose regimens compared to the nontreated controls. However, the LDH concentration did not differ between the standard-therapy and high-dose regimens on those days. Abbreviation: OD₄₉₀, optical density measured at a wavelength of 490 nm.

optimized standard regimen, the composite TTE for combined bacterial subpopulations in the HFS-TB was 27 (95% CI, 23–36) days, which was transformed to a median of 77 (95% CI,

28–135) days in the patients, or about 19.3 weeks on the upper confidence bounds. This is exactly what is seen in the clinic with the optimized treatment regimen in those patients who

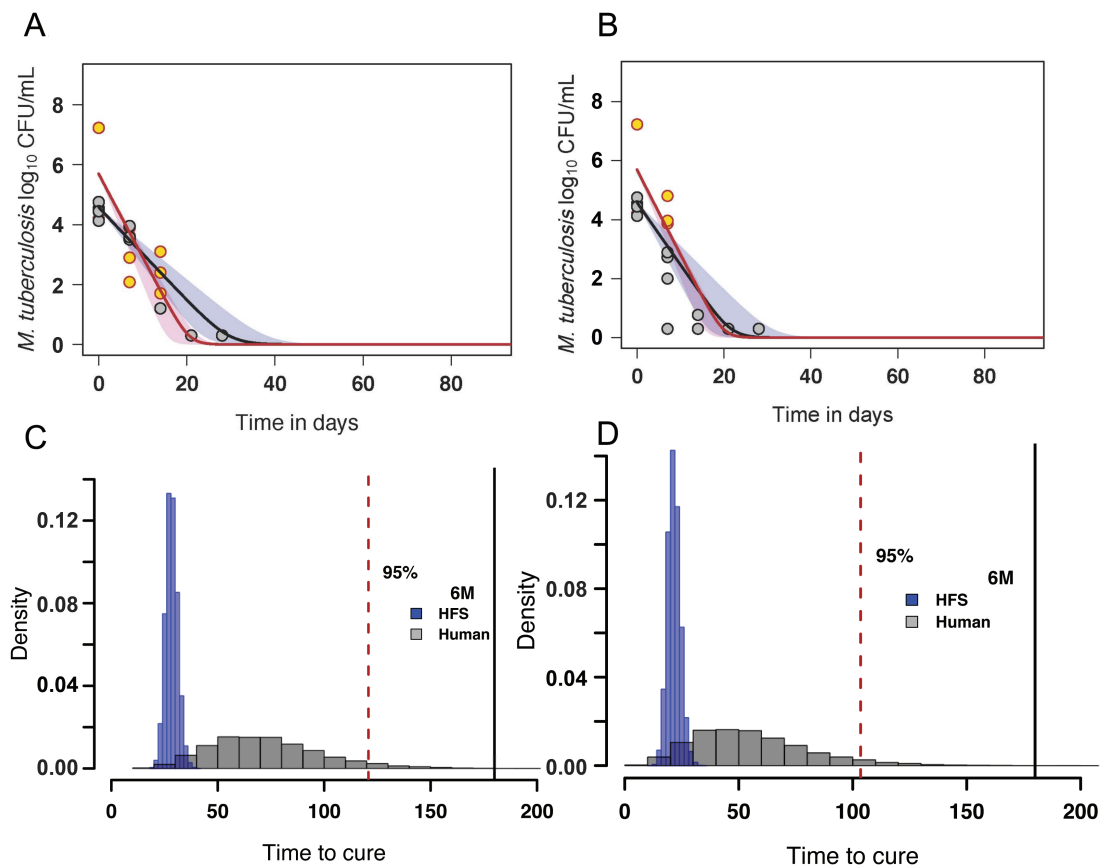


Figure 2. Kill rates of bacilli in the hollow fiber system model of tuberculosis (HFS-TB) and morphism-based transformation to patients. *A*, Kill slopes with the optimized standard regimen that killed 7.23 ± 0.00 log₁₀ colony-forming units (CFU)/mL of the log-phase growth *Mycobacterium tuberculosis* (*Mtb*) and 5.98 ± 0.53 log₁₀ CFU/mL of intracellular *Mtb* in 14 days in the HFS-TB (red circles). However, in the sterilizing activity HFS-TB studies, standard therapy took 28 days to kill 6.92 ± 0.15 log₁₀ CFU/mL semidormant *Mtb* (brown circles). *B*, The high-dose regimen for the same bacillary populations demonstrated faster sterilizing effect (brown circles) compared with the standard regimen. *C*, After transformation from HFS-TB to patients, the distribution of the proportion (density) of the patients with time to extinction (TTE) (x-axis) with standard therapy. *D*, Similarly, after transformation, the distribution of patients with TTE on treatment with the high-dose regimen. The dashed area represents the upper and lower bounds of the 95% confidence interval. Abbreviations: 6M, 6 months; CFU, colony-forming units; HFS, hollow fiber system.

Table 2. Proportion of Patients Cured With the Standard and High-dose Regimens

Regimen	3 Months (95% CrI)	4 Months (95% CrI)	6 Months (95% CrI)
Standard therapy	78.47 (77.65–79.26)	95.25 (94.82–95.65)	99.94 (99.87–99.97)
High-dose regimen	90.06 (89.46–90.63)	99.97 (99.67–98.23)	99.96 (99.9–99.98)

Abbreviation: CrI: credible interval.

achieve faster TTE. **Figure 2D** shows the median TTE of *Mtb* in the HFS-TB with the experimental high-dose combination regimen as 20 (95% CI, 17–30) days. Based on the morphism transformation factor and Latin hypercube sampling, this was transformed to a median TTE of 58 (95% CI, 21–111) days, or about 15.9 weeks on the upper confidence bounds in patients. This is moderately faster than the optimized standard therapy. The proportion of patients cured with the optimized standard regimen vs the high-dose regimen at the end of 3, 4, and 6 months, calculated based on these HFS-TB studies and modeling, were as shown in **Table 2**. The table shows that taking the lower 95% CI bounds, and 95% patient cutoff as acceptable proportion of patients who have reached extinction (ie, worst case scenario), the higher-dose regimen may be able to shorten therapy to 4 months and the standard therapy regimen would stay at 6 months, though most patients are actually cured already at 4 months with the standard regimen in this study.

DISCUSSION

In the present study, we show that a combination of high-dose rifampin at least 3 times the standard dose, and a pyrazinamide dose double the standard dose, and moxifloxacin at 800 mg per day, was associated with faster sterilizing effect based on kill rates achieved in the HFS-TB. Rifampin exposure is known to be dose-related [18, 39], and improved clinical response has been reported with doses up to 1200 mg [40]. Previously, using the HFS-TB and clinical trial simulation, we identified moxifloxacin 800 mg/day as optimal dose for *Mtb* [15]. The faster sterilizing effect meant that there was a possibility of shortening the therapy duration to 4 months with the high-dose regimen, supported by one recent clinical study suggesting that shortening of therapy duration may be achieved by using high-dose rifampin and moxifloxacin [41].

With regard to possible toxicity, there was no significant difference in the LDH levels with our 3D liver KUBES model between the high-dose rifampin and pyrazinamide regimen and optimized standard therapy. The rifampin dose we used was 3 times higher than the dose used in the RIFATOX study (An international multicentre controlled clinical trial to evaluate the toxicity of high dose rifampicin in the treatment of pulmonary tuberculosis, ISRCTN55670677), which was not associated with hepatotoxicity in the clinical trial. In addition, Boeree et al recently reported that rifampin up to 35 mg/kg could be

administered safely [41]. However, none of the clinical studies added high-dose pyrazinamide to the high-dose rifampin, so clinical studies to establish the safety of the 2 drugs at high doses administered together are still to be conducted.

Our study has its own limitations. Perhaps the main limitation is that we gave very high PK/PD exposures of isoniazid and rifampin in the standard regimen (**Table 1**), so the kill slopes were faster than is usually encountered in HFS-TB on this regimen [27]. As a result, on translation a higher proportion of patients had negative TTEs by the fourth month than in the usual standard therapy in patients after our transformation. Indeed, patients on standard therapy with the drug exposures equivalent to those in the HFS-TB have faster sterilizing effect rates and time to negative sputum [38]. Second, in the sterilizing activity HFS-TB studies, the semidormant *Mtb* growth rate was higher than is usually encountered in the HFS-TB for sterilizing effect, which we have reported previously [30]. This could affect the TTE of both the standard-therapy and high-dose regimens. Nevertheless, the TTEs we identified are robust and fall within the range identified on analyzing patients on standard therapy in clinical trials. Thus, our modeling and simulations still predicted a shorter duration of therapy with the high-dose regimen despite this limitation.

In summary, rifampin, pyrazinamide, and moxifloxacin have the potential to improve the efficacy of anti-TB treatment regimens and to shorten the duration of therapy, provided the doses are selected based on PK/PD studies and clinical trial simulations utilizing the MIC distribution of the clinical strains. The safety of increased doses needs to be validated in human clinical trials.

Supplementary Data

Supplementary materials are available at *Clinical Infectious Diseases* online. Consisting of data provided by the authors to benefit the reader, the posted materials are not copyedited and are the sole responsibility of the authors, so questions or comments should be addressed to the corresponding author.

Notes

Author contributions. Conceptualization and design: S. S. and T. G. HFS-TB experiments: D. D., S. S.. PK/PD modeling: T. G. TTE modeling, Latin hypercube sampling, and morphism transformation: G. M. First draft of manuscript: S. S. and T.G. Review and editing: D. D., S. S., G. M., T. G.. Funding acquisition: T. G. Supervision: T. G.

Financial support. This work was supported by the National Institutes of Health (NIH) via the NIH Director New Innovator Award (National Institute of General Medical Sciences, grant number DP2 OD001886, and National Institute of Allergy and Infectious Diseases, grant numbers R01 AI079497 and R56 AI111985 to T. G.).

Supplement sponsorship. This supplement is sponsored by the Baylor Institute of Immunology Research of the Baylor Research Institute.

Potential conflicts of interest. All authors: No reported conflicts. All authors have submitted the ICMJE Form for Disclosure of Potential Conflicts of Interest. Conflicts that the editors consider relevant to the content of the manuscript have been disclosed.

References

1. Dheda K, Gumbo T, Maartens G, et al. The epidemiology, pathogenesis, transmission, diagnosis, and management of multidrug-resistant, extensively drug-resistant, and incurable tuberculosis [manuscript published online ahead of print 15 March 2017]. *Lancet Respir Med* **2017**. doi:10.1016/S2213-2600(17)30079-6.
2. Mitchison DA. Basic mechanisms of chemotherapy. *Chest* **1979**; 76:771–81.
3. Diacon AH, Pym A, Grobusch M, et al. The diarylquinoline TMC207 for multidrug-resistant tuberculosis. *N Engl J Med* **2009**; 360:2397–405.
4. Gler MT, Skripconoka V, Sanchez-Garavito E, et al. Delamanid for multidrug-resistant pulmonary tuberculosis. *N Engl J Med* **2012**; 366:2151–60.
5. Srivastava S, Magombedze G, Koeth T, et al. Linezolid dose that maximizes sterilizing effect while minimizing toxicity and resistance emergence for tuberculosis. *Antimicrob Agents Chemother* **2017**; 61:e00751–17.
6. Deshpande D, Srivastava S, Chapagain M, et al. Ceftazidime-avibactam has potent sterilizing activity against highly drug-resistant tuberculosis. *Sci Adv* **2017**; 3:e1701102.
7. Aung KJ, Van Deun A, Declercq E, et al. Successful 9-month Bangladesh regimen for multidrug-resistant tuberculosis among over 500 consecutive patients. *Int J Tuberc Lung Dis* **2014**; 18:1180–7.
8. Deshpande D, Srivastava S, Nuermberger E, et al. Multiparameter responses to tedizolid monotherapy and moxifloxacin combination therapy models of children with intracellular tuberculosis. *Clin Infect Dis* **2018**; 67(Suppl 3):S342–8.
9. Deshpande D, Srivastava S, Bendet P, et al. Antibacterial and sterilizing effect of benzylpenicillin in tuberculosis. *Antimicrob Agents Chemother* **2018**; 62:e02232–17.
10. Srivastava S, Deshpande D, Nuermberger E, Cirrincione KN, Dheda K, Gumbo T. The sterilizing effect of tedizolid for pulmonary tuberculosis. *Clin Infect Dis* **2018**; 67(Suppl 3):S336–41.
11. Gillespie SH, Crook AM, McHugh TD, et al; REMoxTB Consortium. Four-month moxifloxacin-based regimens for drug-sensitive tuberculosis. *N Engl J Med* **2014**; 371:1577–87.
12. Merle CS, Fielding K, Sow OB, et al; OFLOTUB/Gatifloxacin for Tuberculosis Project. A four-month gatifloxacin-containing regimen for treating tuberculosis. *N Engl J Med* **2014**; 371:1588–98.
13. Pasipanodya JG, Smythe W, Merle CS, et al. Three-way concentration-dependent antagonism of gatifloxacin, pyrazinamide, and rifampicin during treatment of pulmonary tuberculosis. *Clin Infect Dis* **2018**; 67(Suppl 3):S284–92.
14. Alffenaar JW, Gumbo T, Aarnoutse R. Shorter moxifloxacin-based regimens for drug-sensitive tuberculosis. *N Engl J Med* **2015**; 372:576.
15. Gumbo T, Louie A, Deziel MR, Parsons LM, Salfinger M, Drusano GL. Selection of a moxifloxacin dose that suppresses drug resistance in *Mycobacterium tuberculosis*, by use of an in vitro pharmacodynamic infection model and mathematical modeling. *J Infect Dis* **2004**; 190:1642–51.
16. Deshpande D, Pasipanodya JG, Srivastava S, et al. Gatifloxacin pharmacokinetics/pharmacodynamics-based optimal dosing for pulmonary and meningeal multidrug-resistant tuberculosis. *Clin Infect Dis* **2018**; 67(Suppl 3):S274–83.
17. Deshpande D, Pasipanodya JG, Mpagama SG, et al. Levofloxacin pharmacokinetics/pharmacodynamics, dosing, susceptibility breakpoints, and artificial intelligence in the treatment of multidrug-resistant tuberculosis. *Clin Infect Dis* **2018**; 67(Suppl 3):S293–302.
18. Gumbo T, Louie A, Deziel MR, et al. Concentration-dependent *Mycobacterium tuberculosis* killing and prevention of resistance by rifampin. *Antimicrob Agents Chemother* **2007**; 51:3781–8.
19. Boeree MJ, Diacon AH, Dawson R, et al; PanACEA Consortium. A dose-ranging trial to optimize the dose of rifampin in the treatment of tuberculosis. *Am J Respir Crit Care Med* **2015**; 191:1058–65.
20. Kreis B, Pretet S, Birenbaum J, et al. Two three-month treatment regimens for pulmonary tuberculosis. *Bull Int Union Tuberc* **1976**; 51:71–5.
21. Pasipanodya JG, McIlleron H, Burger A, Wash PA, Smith P, Gumbo T. Serum drug concentrations predictive of pulmonary tuberculosis outcomes. *J Infect Dis* **2013**; 208:1464–73.
22. Grosset J, Truffot-Pernot C, Lacroix C, Ji B. Antagonism between isoniazid and the combination pyrazinamide-rifampin against tuberculosis infection in mice. *Antimicrob Agents Chemother* **1992**; 36:548–51.
23. Grosset J. The sterilizing value of rifampicin and pyrazinamide in experimental short-course chemotherapy. *Bull Int Union Tuberc* **1978**; 53:5–12.
24. Sahota T, Della Pasqua O. Feasibility of a fixed-dose regimen of pyrazinamide and its impact on systemic drug exposure and liver safety in patients with tuberculosis. *Antimicrob Agents Chemother* **2012**; 56:5442–9.
25. Srivastava S, Pasipanodya JG, Ramachandran G, et al. A long-term co-perfused disseminated tuberculosis-3D liver hollow fiber model for both drug efficacy and hepatotoxicity in babies. *EBioMedicine* **2016**; 6:126–38.
26. Rosenthal IM, Zhang M, Williams KN, et al. Daily dosing of rifampentine cures tuberculosis in three months or less in the murine model. *PLoS Med* **2007**; 4:e344.
27. Magombedze G, Pasipanodya JG, Srivastava S, Deshpande D, McIlleron H, Gumbo T. Transformation morphisms and time-to-extinction analysis that map therapy duration from preclinical models to patients with tuberculosis: translating from apples to oranges. *Clin Infect Dis* **2018**; 67(Suppl 3):S349–58.
28. Gumbo T, Dona CS, Meek C, Leff R. Pharmacokinetics-pharmacodynamics of pyrazinamide in a novel in vitro model of tuberculosis for sterilizing effect: a paradigm for faster assessment of new antituberculosis drugs. *Antimicrob Agents Chemother* **2009**; 53:3197–204.
29. Gumbo T, Alffenaar JC. Pharmacokinetics/pharmacodynamics background and methods and scientific evidence base for dosing of second-line tuberculosis drugs. *Clin Infect Dis* **2018**; 67(Suppl 3):S267–73.
30. Musuka S, Srivastava S, Siyambalapitiyage Dona CW, et al. Thioridazine pharmacokinetic-pharmacodynamic parameters “wobble” during treatment of tuberculosis: a theoretical basis for shorter-duration curative monotherapy with congeners. *Antimicrob Agents Chemother* **2013**; 57:5870–7.
31. Gumbo T, Pasipanodya JG, Nuermberger E, Romero K, Hanna D. Correlations between the hollow fiber model of tuberculosis and therapeutic events in tuberculosis patients: learn and confirm. *Clin Infect Dis* **2015**; 61(Suppl 1):S18–24.
32. Deshpande D, Srivastava S, Nuermberger E, Pasipanodya JG, Swaminathan S, Gumbo T. A faropenem, linezolid, and moxifloxacin regimen for both drug-susceptible and multidrug-resistant tuberculosis in children: FLAME path on the Milky Way. *Clin Infect Dis* **2016**; 63:S95–101.
33. D’Argenio DZ, Schumitzky A. ADAPT II. A program for simulation, identification, and optimal experimental design. User manual. Biomedical simulations resource. Los Angeles: University of Southern California, **1997**.
34. Srivastava S, Pasipanodya JG, Meek C, Leff R, Gumbo T. Multidrug-resistant tuberculosis not due to noncompliance but to between-patient pharmacokinetic variability. *J Infect Dis* **2011**; 204:1951–9.
35. Iman RL. Latin hypercube sampling. *Encyclopedia of quantitative risk analysis and assessment*. Wiley Online Library: John Wiley & Sons, Ltd, **2008**.
36. Rockwood N, Pasipanodya JG, Denti P, et al. Concentration-dependent antagonism and culture conversion in pulmonary tuberculosis. *Clin Infect Dis* **2017**; 64:1350–9.
37. Gumbo T, Louie A, Liu W, et al. Isoniazid bactericidal activity and resistance emergence: integrating pharmacodynamics and pharmacogenomics to predict efficacy in different ethnic populations. *Antimicrob Agents Chemother* **2007**; 51:2329–36.
38. Chigutsa E, Pasipanodya JG, Visser ME, et al. Impact of nonlinear interactions of pharmacokinetics and MICs on sputum bacillary kill rates as a marker of sterilizing effect in tuberculosis. *Antimicrob Agents Chemother* **2015**; 59:38–45.
39. McIlleron H, Wash P, Burger A, Norman J, Folb PI, Smith P. Determinants of rifampin, isoniazid, pyrazinamide, and ethambutol pharmacokinetics in a cohort of tuberculosis patients. *Antimicrob Agents Chemother* **2006**; 50:1170–7.
40. Diacon AH, Patientia RF, Venter A, et al. Early bactericidal activity of high-dose rifampin in patients with pulmonary tuberculosis evidenced by positive sputum smears. *Antimicrob Agents Chemother* **2007**; 51:2994–6.
41. Boeree MJ, Heinrich N, Aarnoutse R, et al; PanACEA Consortium. High-dose rifampicin, moxifloxacin, and SQ109 for treating tuberculosis: a multi-arm, multi-stage randomised controlled trial. *Lancet Infect Dis* **2017**; 17:39–49.